

Adsorption of Trace Metals on the Natural Amorphous Iron Oxyhydroxide from the Taebag Coal Mine Area

태백 탄전 지대의 비정질 철 수산화물에 대한 희귀원소의 흡착

Jae-Young Yu (유재영) * · In-Kyu Choi (최인규) *

Abstract : To determine the apparent equilibrium constants, $K_{ad,app}$, for the adsorption reactions of trace metals on amorphous iron oxyhydroxide (AIO) in the Taebag coal mine area, time-adsorption and pH-adsorption experiments were performed for a selected bottom sediment mainly comprised of AIO from the study area. The results from the adsorption experiments indicate that most of the trace metals, except Pb, achieve equilibrium states with AIO and thus, the calculated $K_{ad,app}$ may represent the true apparent equilibrium constants. $K_{ad,app}$ and the stoichiometric coefficients of proton, x , of the adsorption reactions between the trace metals and AIO were respectively calculated from the intercepts and slopes of the regression lines of $\log(\Gamma/[M]_{aq})$ against pH provided by pH-adsorption experiments. The calculated $K_{ad,app}$ of this study has the values of the range from 10^{+5} to $10^{2.75}$, which is much different from the reported values by other investigators for simple experimental systems. $K_{ad,app}$ of this study is more or less close but not exactly pertinent to the estimated values for the other natural systems. It indicates that $K_{ad,app}$ for the adsorption reactions in the aquatic system in the study area is unique and thus should be determined before the adsorption modelling. The calculated x of this study has the values of the range from -0.3 to 0.7, which is also much different from what most geochemists generally accept. The discrepancy in x may be due to the competition among different kinds of ionic species on the adsorption site or simultaneous occurrence of different kinds of adsorption reactions. The results from this study should help construct an appropriate adsorption model for the aquatic systems polluted by the coal mine drainage in the Taebag area. With the constructed model, one can describe the concentration variations of trace metals due to the adsorption in the system, which is an essential part of the investigation on the water quality affected by coal mine drainage in the Taebag coal field.

KEY WORDS : Adsorption, Amorphous Iron Oxyhydroxide, Trace Elements, Apparent Equilibrium Constant, Stoichiometric Coefficient of Proton.

요 약 : 태백 탄전 지대에서 산출되는 비정질 철 수산화물 (AIO)에 대한 희귀 원소 흡착 반응의 총체적 평형 상수 $K_{ad,app}$ 를 계산하기 위해 시간-흡착 실험 및 pH-흡착 실험을 실시하였다. 이와 같은 두 실험 결과에 의하면, Pb를 제외한 모든 원소의 흡착 반응이 평형에 도달하여 계산된 $K_{ad,app}$ 값이 실제의 값일 가능성이 높음을 알 수 있다. 희귀 원소와 AIO간의 흡착 반응에 대한 $K_{ad,app}$ 와 수소 이온의 반응 계수 x 는 pH-흡착 실험 결과로부터 얻어진 $\log(\Gamma/[M^{2+}]_{aq})$ 와 pH에 대한 선형 회귀 식의 절편과 기울기로부터 계산되었다. 이 연구에서 계산된 $K_{ad,app}$ 는 10^{+5} 에서 $10^{2.75}$ 범위의 값을 갖는데, 이는 다른 연구자들에 의한 단순 조성계에 대한 실험 결과와 많은 차이를 보인다. 이 연구에 의한 $K_{ad,app}$ 는 자연계의 다른 환경에서 평가된 것과 어느 정도 비슷한 값을 보이지만 정확히 일치하지는 않는다. 이러한 사실은 연구 지역의 수계에서 $K_{ad,app}$ 가 독특한 그만의 값을 갖는 것을 나타내므로, 흡착 모델링 전에 반드시 연구 지역의 수계에 맞는 정확한 $K_{ad,app}$ 값이 평가되어야 함을 의미한다. 이 연구에 의한 x 는 -0.3 내지 0.7의 값을 갖는데, 이 또한 일반적으로 지구화학자들 사이에서 받아들여지는 값과는 상당히 다른 것이다. 이러한 x 값의 차이는 아마도 흡착 자리에 대한 다른 이온종간의 경쟁 또는 종류가 다른 여러 흡착 반응의 동시 진행에 의한 것으로 생각된다. 이 연구의 결과는 태백 지역에서 탄광 폐수에 오염된 수계 내에서의 적절한 흡착 모델을 세우는데 도움을 줄 것이다. 이렇게 세워진 흡착 모델을 이용하여 수계 내에서의 흡착에 따른 금속 원소 함량 변화를 기술할 수 있을 것이며, 이는 태백 탄전 지역에서 광산 폐수가 수질에 미치는 영향에 대한 연구에 중요한 부분이 될 것이다.

주요어 : 흡착, 비정질 철 수산화물, 희귀 원소, 총체적 평형 상수, 수소 이온 반응 계수

*Department of Geology, College of Natural Sciences, Kangwon National University, Chuncheon, Kangwon-Do 200-701(강원대학교 지질학과)

INTRODUCTION

Coal mine drainage generally contains relatively high concentrations of toxic trace metals due to its low pH and the presence of abundant ligands. Environmentally the behavior of these toxic metals along downstreams have attracted a great deal of interest not only from scientists but also from the water consumers who may drink it or use it for agricultural purposes. Geochemists have tried to describe and predict the behavior of the metals from mine drainage in terms of their precipitation, dissolution, complexation, and adsorption processes and had some successful cases of doing so (Nordstrom *et al.*, 1979; Fuge *et al.*, 1991; Brown, 1991; Sanden, 1991). Thanks to numerous internally consistent thermodynamic data bases (Helgeson *et al.*, 1978; Robie *et al.*, 1978) and computer programs (see Faure (1991) for the list), geochemists now easily describe the precipitation, dissolution and complexation of metals. However, describing adsorption of trace metals is still a relatively difficult task, because there is no universally applicable single adsorption model.

Aware of the importance of the role of adsorption reactions in the transport and ultimate fate of the trace metals in many aquatic systems, geochemists have proposed several models and tried to explain the adsorption behavior of trace metals in natural aquatic systems. Among these, the widely accepted ones are empirical distribution models, isotherm models, and electric double layer models (Davis and Kent, 1990). Each model requires its own empirically determined parameters to account the adsorption behavior of trace metals. With the empirical parameters determined from experiments, the models can describe most of the adsorption properties of trace metals in relatively simple systems. However, these parameters are often not applicable to the natural systems due to its much more complex nature. Adsorption of trace metals depends on the kinds and amounts of adsorbate and adsorbent, presence of other competing adsorbate and adsorbent, ratio of adsorbate to adsorbent, and ionic strength of the solution (Davis and Kent, 1990). In most cases, natural systems consist of several kinds of adsorbate and adsorbent and show various ionic strength. Thus, one has to identify the kinds of adsorbate and adsorbent, analyze the chemical composition of the system, and then determine the appropriate parameters for the selected model before describing or predicting the fate of the trace elements in natural systems.

The purpose of this study is to determine one of the most important model parameters, namely "apparent equilibrium constant, $K_{ad,app}$, for the adsorption of trace metals on

amorphous iron oxyhydroxide (AIO) from the coal mine drainage in Taebag area. Many closed coal mines are concentrated in the Taebag area and drain significant amount of polluted water into the peripheral streams. The pollution of the streams from the closed coal mines has almost entirely destroyed the aquatic ecosystem as well as made the streams look aesthetically bad by precipitating AIO. For these reasons, urgently required has been a detailed and systematic investigation on the influence of coal mine drainage upon the stream water quality. This study is performed to fulfill the purpose of such investigations by providing informations on the behavior of toxic metals during downstream transport.

THEORY

Adsorption of a metal species on a solid surface is generally represented by



The equilibrium constant, K_{ad} , for reaction (1) becomes

$$K_{ad} = \frac{[\equiv\text{SOM}][\text{H}^+]^x}{[\equiv\text{SOH}_x][\text{M}^{2+}]_{\text{aq}}}, \quad (2)$$

where $\equiv\text{SOM}$ and $\equiv\text{SOH}_x$ are respectively the adsorbed and free solid surface sites and the brackets represent the concentration of the species. For AIO, the adsorption density, Γ , can be written as

$$\Gamma = \frac{[\equiv\text{SOM}]}{\text{Fe}_T}, \quad (3)$$

where Fe_T is the total concentration of iron present as oxyhydroxide. Assuming that the total concentration of site is equal to that of free site, $[\equiv\text{SOH}_x]$, then

$$[\equiv\text{SOH}_x] = n\text{Fe}_T, \quad (4)$$

where n is the number of moles of sites per mole of AIO. From equations (2), (3), and (4)

$$\log \frac{\Gamma}{[\text{M}^{2+}]_{\text{aq}}} = \log(K_{ad} \cdot n) + xpH. \quad (5)$$

Equation (5) is a linear equation. Thus, if we plot $\log(\Gamma/[\text{M}^{2+}]_{\text{aq}})$ against pH , K_{ad} and x can be simultaneously obtained from the slope and intercept of the line.

METHODS

Sample Collection and Preparation

Stream water and bottom sediment samples, which are supposed to reach an equilibrium state with each other, were collected at several sites in the studied area on April, 1994.

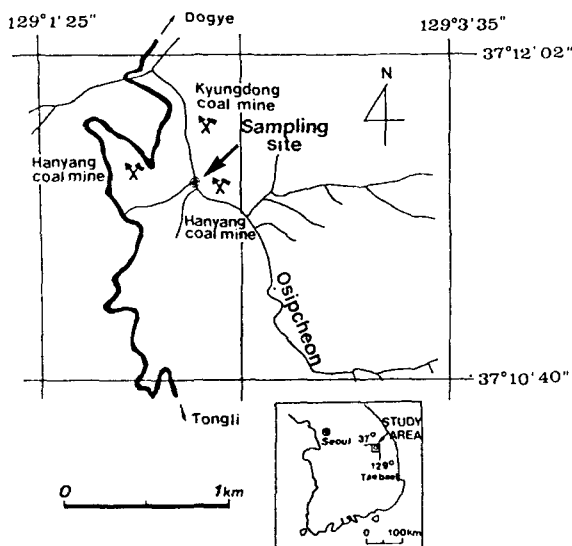


Figure 1. The location of the sampling site of TAS-8

Each water sample was divided into two portions and one portion (P-I) was filtered and acidified and the other portion (P-II) was only filtered into 1 L pre-soaked polyethylene bottles. Filtering and acidification of the water samples used 0.1 μm micropore filter and 1 N HNO_3 , respectively. The bottom sediments were scooped with a flat plastic sampling tool and transferred to a 1 L pre-washed plastic bottle. All the samples were brought to laboratory and stored in a refrigerator for various analyses.

For the purpose of this study, we selected appropriate one pair of water and bottom sediment, TAS-8, from the above samples and perform the necessary experiments on the selected sample (see below for the reason of sample selection).

Identification of Adsorbent

To identify the kind of adsorbent in stream water, collected bottom sediments were analyzed with XRD and XRF. XRD and XRF analyses showed that the possible adsorbents are AIO, chlorite, kaolinite, and Mn-hydroxide. To eliminate the complexity caused by composite adsorbent, the bottom sediment (TAS-8) almost entirely consisting of AIO was selected to perform further sorption experiment in this study. The location of the sampling site of TAS-8 is shown in Figure 1.

Sorption Experiments

Time-Adsorption experiment; To examine if the sorption reactions reach an equilibrium state, 1 g of dried TAS-8 was mixed with 300 mL of the corresponding P-II water sample. The mixture was then adjusted to pH 4.5 with 1N HCl and mixed thoroughly on a mechanical shaker. A portion of the mixture was periodically extracted with 10 mL

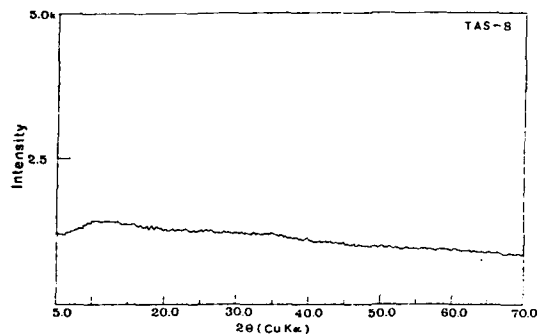


Figure 2. The XRD pattern of TAS-8, obtained with Rigaku x-ray diffractometer (Model RAD-III-C) under the conditions of 40 KV and 30 mA for the x-ray generation, 1-0.15-1 degrees for the slits, and 1 degrees/min for the scan speed.

pipet at each 30 minute interval, filtered with 0.1 μm micropore filter, acidified with 1 N HNO_3 , and stored for later chemical analyses.

pH-Adsorption experiment; To investigate the adsorption properties of AIO from the study area as a function of pH, another 1 g of dried TAS-8 was mixed with 300 mL of the corresponding P-II water sample. The mixture was thoroughly homogenized and divided into five portions. Each portion was transferred into a 50 mL polyethylene vial and adjusted to an appropriate pH with 0.1 N HCl and 0.1 N NaOH. The initial adjusted pH were 3.0, 5.0, 6.0, 7.0, and 9.0. After shaking for 16 hours, the final pH's of the mixtures were measured; they are pH 2.84, 5.29, 6.50, 7.41, and 9.13, respectively. The mixtures were then filtered and the filtrates were acidified to be stored until later chemical analyses. The filter cake were dissolved with 50 mL 1N HCl and filtered again. The residues were discarded and the filtrates were again acidified for later chemical analyses.

Analyses

The temperature, pH, E_H , and conductivity of water samples are measured in the field. Major components of TAS-8 and the corresponding water sample were analyzed with XRF and ICP-AES, respectively. Anion analyses of P-II water samples were carried out with IC. Trace element analyses of P-I water samples and all the filtrates were carried out with ICP-MS and ICP-AES. All of the above chemical analyses were performed in the laboratory of Korea Basic Science Center at Seoul.

RESULTS AND DISCUSSION

Figure 2 and Table 1 respectively show the XRD pattern and the chemical composition of TAS-8, suggesting that it is almost entirely comprised of AIO. The AIO of TAS-8 shows

Table 1. The chemical composition of sediment TAS-8

Major elements in oxide forms (wt.%) ^a		Minor elements (ppm) ^b	
SiO ₂	5.19	Li	1.376
Al ₂ O ₃	2.00	Cr	13.673
Fe ₂ O ₃	78.65	Co	98.321
TiO ₂	0.01	Ni	143.022
MnO ₂	0.21	Cu	36.761
CaO	2.03	Zn	1132.120
MgO	0.21	Rb	108.817
K ₂ O	0.05	Sr	453.858
Na ₂ O	N.D ^d	Cd	0.919
P ₂ O ₅	0.03	Ba	126.719
L.O.I. ^c	12.03	U	15.927
		As	37.940
		Se	51.920
Total	100.41		

a : Analyzed with XRF.
 b : Analyzed with ICP-MS.
 c : L.O.I. = Loss of ignition.
 d : N.D = Not detected.

dark red color, while most AIO are reportedly yellowish. Anderson and Benjamin (1985) speculated that the AIO of dark red color might be actually microcrystalline aggregates of goethite. However, authors do not agree with Anderson and Benjamin, because if it is microcrystalline aggregates of goethite, it should show some peaks under very intensive and slow scan of x-rays. TAS-8 doesn't show any difference from Figure 1 even under very slow and intensive x-ray scan.

Table 2 compares the chemical composition of the stream water at the site of TAS-8 with that of world average fresh water from Livingstone (1963). The stream water from the study area has higher concentrations of most components, especially SO₄ and trace elements, than the average fresh water.

Figure 3 shows the results of time-adsorption experiments, suggesting that the reactions between AIO and Ni, Cu, Zn, Cd, and U may be regarded to reach an equilibrium state within the experiment time span. However, Cr, Co, and Pb are not equilibrated with AIO within 400 min. Thus, the calculated K_{ad} for Cr, Co, and Pb with equation (5) may not represent the true values, although pH-adsorption experiments allowed the mixtures to react for 16 hours which is much longer than the time span of the time-adsorption experiment.

Table 3 summarizes the chemical compositions of the filtrates and filter cakes from the pH-adsorption experiments. Before interpreting the experimental results, it is necessary to ensure that the variations in chemical compositions of filtrate are principally caused by adsorption reaction at different pH. For this purpose, a few authors have plotted the total dissolved concentration of a metal against pH of the solution on the solubility diagram as shown in Figure 4 (Johnson,

Table 2. Comparison of the chemical composition (mg/L) of the stream water at the site of TAS-8 with that of the world average fresh water from Livingstone(1963).

	TAS-8	World average fresh water
Na	3.909	6.3
Mg	45.400	4.1
Al	0.062	0.4
K	3.973	2.3
Ca	78.828	15.0
SiO ₂	0.015	13.1
Cl ⁻	4.41	7.8
NO ₃ ⁻	5.19	-
SO ₄ ²⁻	495.175	11.2
CO ₃ ²⁻	0.133	-
HCO ₃ ⁻	65.775	58.4
Li	25.08x10 ⁻³	3.0x10 ⁻³
Cr	3.15x10 ⁻³	1.0x10 ⁻³
Co	18.93x10 ⁻³	0.1x10 ⁻³
Ni	24.09x10 ⁻³	0.3x10 ⁻³
Cu	5.96x10 ⁻³	7.0x10 ⁻³
Zn	20.31x10 ⁻³	20.0x10 ⁻³
Rb	330.63x10 ⁻³	1.0x10 ⁻³
Sr	1445.01x10 ⁻³	70.0x10 ⁻³
Cd	0.60x10 ⁻³	-
Ba	18.60x10 ⁻³	20.0x10 ⁻³
u	5.94x10 ⁻³	0.04x10 ⁻³
As	160.00x10 ⁻³	2.0x10 ⁻³
Se	260.00x10 ⁻³	0.2x10 ⁻³
Fe	3900.00x10 ⁻³	670.0x10 ⁻³
Temperature(°C)		10.8
pH		7.42
Eh		270.0
Specific conductivity(μS) at 25°C		818.0
Alkalinity(mg/L as CaCO ₃)		54.06

1986). If significant amount of ligands presents, however, we should plot the total activities of the corresponding species instead of the total concentrations to examine any possible precipitation. The speciations of a solution component and its species activities can be easily calculated by any equilibrium analysis program such as MINTQA2 (Allison *et al.*, 1991). Figure 4 suggests that simply plotting total concentrations of Ni, Zn, Cu, and Cd against pH (solid circles) indicates precipitation of these metals occur in the filtrates of higher pH. However, plotting the activity sum of corresponding species against pH (open circles in Figure 4) indicates the filtrates are undersaturated to the corresponding solids in the pH range of the pH-adsorption experiments. Although Figure 4 represents the stability field only of Ni, Cu, Zn, and Cd, all the filtrates from pH-adsorption experiments are undersaturated for any metal compounds. Thus, the metal

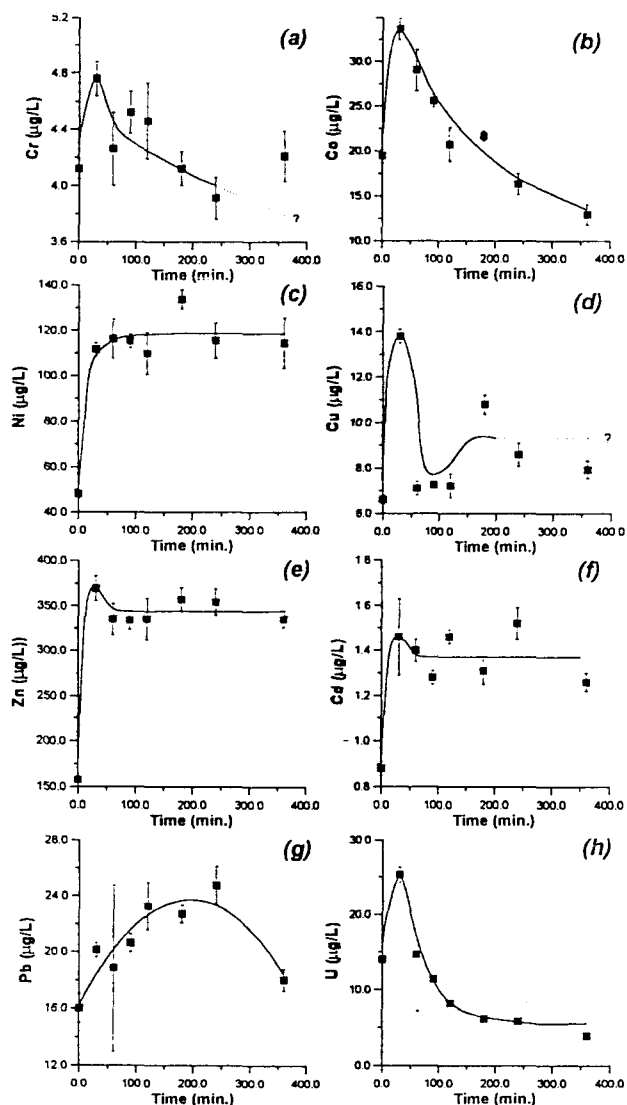


Figure 3. The variations of the metal concentrations as a function of time in the filtrates from the time adsorption experiments.

concentration of the filtrates are principally controlled by adsorption processes.

Figure 5 shows species distributions of the trace metals as a function of pH. As shown in Figure 5, the trace metals exist as more than two species (charged or uncharged) simultaneously at any given pH. On the other hand, equation (5) is valid for only one charged species. This contradiction may be resolved by substituting "an apparent equilibrium constant, $K_{d,app}$ " for K_d in equation (5). Then, $K_{d,app}$ expresses the law of mass action between sum of the charged species of the metal and AIO surface. Note that $K_{d,app}$ become meaningless if a metal has significant amount both of cationic and anionic species at the same time. Fortunately, Figure 5 indicates that this case rarely happens.

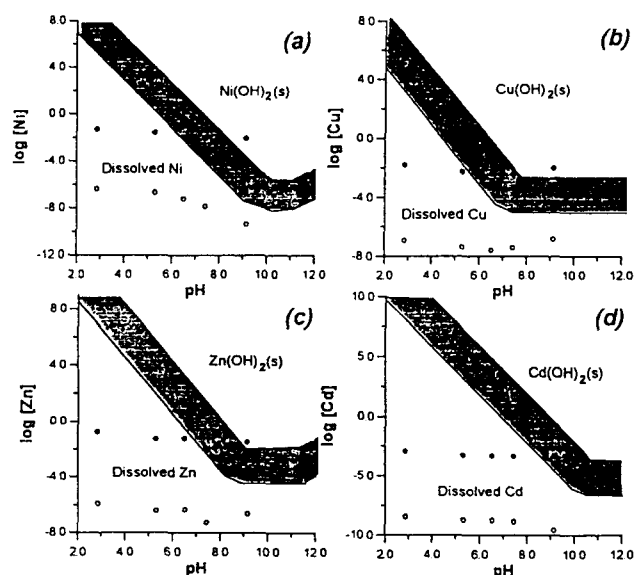


Figure 4. Solubility diagrams of Ni, Cu, Zn and Cd. The solid and open circles represent the data points corresponding to the total concentrations and the activity sums of the species of the trace metals.

Before making a plot of $\log(\Gamma/[M^{2+}]_{aq})$ against pH, the fraction of ionic species of each metal must be first calculated for given pH. Table 4 lists the kinds of the species and their fractions of each metal, which are obtained from MINTQA2. Then, $[M^{2+}]_{aq}$ in equation (5) becomes $[M]_{aq}$, the value of the total concentration of the metal multiplied by the fraction of its ionic species.

Figure 6 shows the plot of equation (5) with the data from Table 3 and Table 4. The linear regression line in Figure 6(a) (Cr) and in Figure 6(h) (U) excluded the first data point at $\text{pH}=2.84$, because the first point represents very different ionic species (Cr^{3+} for Cr and UO_2^{2+} for U) from the rest of the species (refer to Figure 5(a) and 5(h)). Most of the data except those in Figure 6(g) (Pb) show good correlation. The poor correlation in Figure 6(g) may be due to nonequilibrium state between Pb and AIO as suggested in Figure 2(g). Note that the slope of the regression line in Figure 6(h) is opposite to the rest. This is because U mainly presents as oxyanions for experimental pH range (Figure 5(h)), while others are speciated to the positive forms (Figure 5(a) to Figure 5(g)). Figure 6(e) shows two regression lines: One is the regression line for all the data points and the other one is for the data points except the last one at $\text{pH}=9.13$. The last data point is due to the adsorption of $\text{Zn}(\text{CO}_3)_2$, while others due to the adsorption of the cationic species.

To calculate $K_{d,app}$ from the intercepts of the regression lines in Figure 6, required is the mole number of adsorption sites, n , per mole of AIO. With known n ,

Table 3. The chemical compositions($\mu\text{g}/\text{L}$) of the filtrates and filtercakes from the pH-adsorption experiments.

a. filtrate

pH	2.84	5.29	6.50	7.41	9.13
Cr	5.43	3.74	3.41	4.36	4.63
Mn	703.68	330.50	134.68	55.51	20.56
Co	31.41	5.26	1.42	0.73	0.49
Ni	48.00	24.69	9.53	8.33	7.75
Cu	14.51	5.33	3.76	3.62	9.76
Zn	162.75	49.62	57.32	8.07	31.71
Cd	1.04	0.48	0.42	0.39	0.40
Pb	1.94	3.80	8.77	1.45	4.70
U	67.94	0.79	0.68	1.48	3.89
Mg	34.20 x10 ³	37.30 x10 ³	39.70 X10 ³	32.60 x10 ³	30.20 x10 ³
Ca	120.00 x10 ³	132.40 x10 ³	145.80 x10 ³	111.20 x10 ³	99.10 x10 ³
Sr	1.50 x10 ³	1.50 x10 ³	1.70 x10 ³	1.10 x10 ³	0.90 x10 ³
Fe	6.18 x10 ³	n.d [*]	0.65 x10 ³	n.d	0.11 x10 ³
Na	5.01 x10 ³	5.02 x10 ³	5.11 x10 ³	5.02 x10 ³	5.02 x10 ³
K	3.40 x10 ³	2.71 x10 ³	2.63 x10 ³	2.82 x10 ³	3.11 x10 ³
Si	7.95 x10 ³	4.04 x10 ³	2.31 x10 ³	1.42 x10 ³	0.90 x10 ³
Cl ⁻	211.93 x10 ³	73.40 x10 ³	38.49 x10 ³	23.05 x10 ³	10.05 x10 ³
NO ₃	26.23 x10 ³	27.92 X10 ³	27.90 x10 ³	24.87 x10 ³	29.07 x10 ³
SO ₄ ²⁻	247.64 x10 ³	270.21 x10 ³	196.36 x10 ³	300.64 x10 ³	298.36 x10 ³

b. filter cake

pH	2.84	5.29	6.50	7.41	9.13
Cr	289.74	310.82	307.80	306.33	300.96
Mn	1572.65	1954.56	770.35	3314.58	3421.9
Co	64.46	90.67	283.22	137.05	139.77
Ni	751.38	772.55	998.04	840.03	899.58
Cu	79.98	111.24	143.70	112.98	106.78
Zn	187.74	1235.91	3696.81	1852.53	1701.62
Cd	42.60	45.42	43.62	36.06	37.98
Pb	29.71	35.94	59.89	35.58	32.24
U	21.96	89.56	39.76	129.81	131.77
Mg	0.47 10 ³	0.60 x10 ³	2.61 x10 ³	1.88 x10 ³	3.15 x10 ³
Ca	1.79 x10 ³	3.87 x10 ³	28.69 x10 ³	18.54 x10 ³	25.63 x10 ³
Sr	0.09 x10 ³	0.17 x10 ³	1.28 x10 ³	0.70 x10 ³	0.85 x10 ³
Fe	579.30 x10 ³	524.90 x10 ³	1882.10 x10 ³	857.20 x10 ³	901.10 x10 ³
Na	5.20x10 ³	5.20x10 ³	5.79x10 ³	5.32x10 ³	5.37x10 ³
K	0.56 x10 ³	0.57 x10 ³	0.49 x10 ³	0.63 x10 ³	0.46 x10 ³
Si	12.61 x10 ³	16.22 x10 ³	66.91 x10 ³	27.63 x10 ³	28.86 x10 ³

*n.d : Not detected.

$$\log(K_{sd,app}) = \text{intercepts} - \log(n). \quad (6)$$

Several investigators determined n values, but widely accepted values may be those of Davis and Leckie (1978) (n= 1.75) and Dzombak and Morrel (1990) (n= 0.1 to 0.9). Table 5 compares the $K_{sd,app}$ values calculated with equation (6) of this study with those reported by other investigators. The $K_{sd,app}$ values of Kinniburgh and Jackson (1982), Davis and Leckie (1978), Benjamin and Leckie (1981), and Dzombak and Morrel (1990) were obtained from laboratory

experiments of simple systems. On the other hand, Tessier *et al.* (1985)'s $K_{sd,app}$ values were estimated from the analyses of the pore water and oxic sediments in Clearwater Lake, Joe Lake, and Fairbank Lake. It may be noted from Table 5 that $K_{sd,app}$ values of this study are much different from those obtained with simple experiments, indicating that the simple adsorption experimental results can't be applied to the complex natural aquatic systems like that of this study. The values of $K_{sd,app}$ are more or less close but not pertinent to the values of Tessier *et al.* It suggests that one must determine

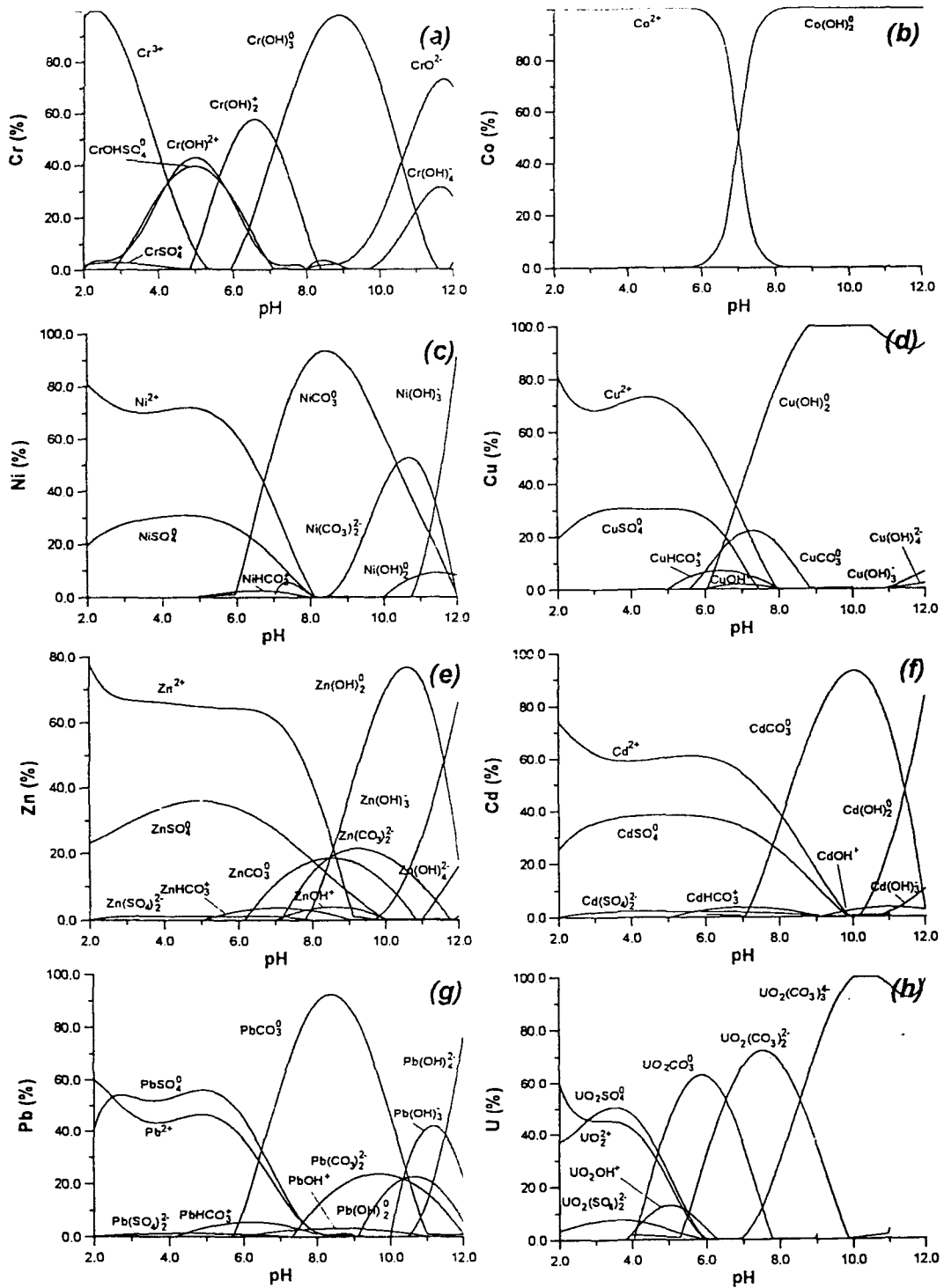


Figure 5. The species distributions of the trace metals as a function of pH.

one's own $K_{ad,app}$ appropriate to the interested natural systems before adsorption modelling. The difference in $K_{ad,app}$ values between this study and Tessier *et al.*'s may be due to the different amount of adsorbent and different metal concentrations between them.

The slopes of the regression lines, x , in Figure 6 (except

Figure 6(g) and Figure 6(h)) suggest that the stoichiometric coefficient of proton in reaction (1) has the range of 0.13 to 0.71. Generally x has the values near to 1.0 or 2.0 (Benjamin and Leckie, 1981; Johnson, 1986). Although the reason for the discrepancies in x values between this study and others is not clear, it may be caused by the competition in

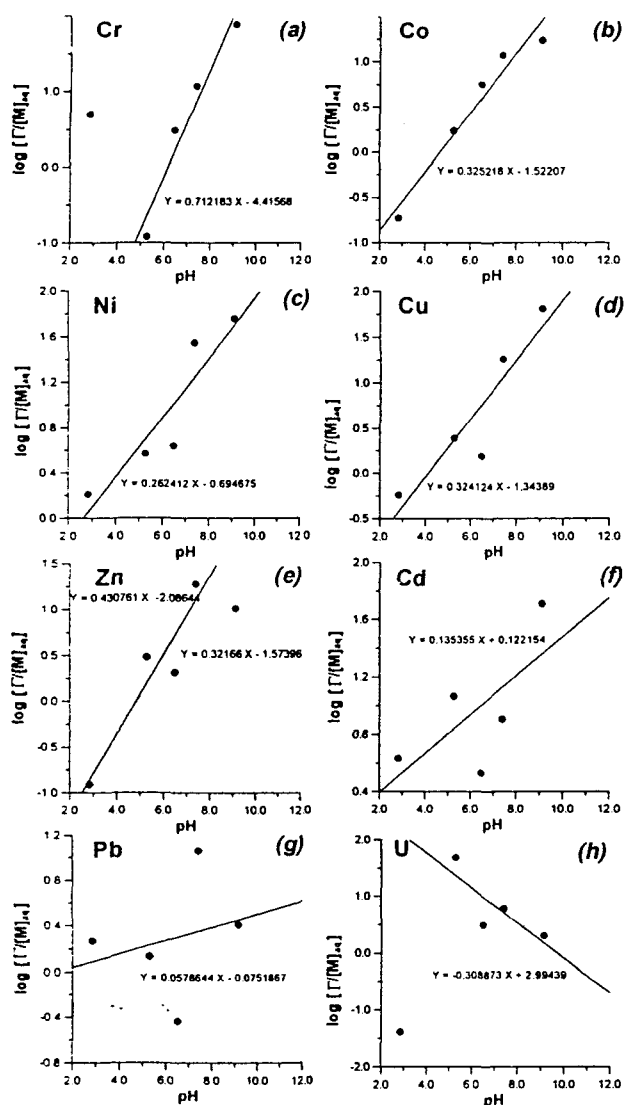
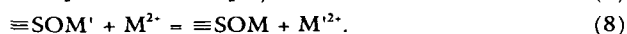


Figure 6. Plot of $\log(\Gamma/[M]_{aq})$ against pH. The solid circles are the data points calculated from Table 3 and Table 4. The solid lines represent the linear regression lines.

adsorption among the different kinds of the trace metals or by the different kinds of surface reaction from reaction (1). Benjamin and Leckie (1981), Millward and Moore (1982), and Benjamin (1983) discussed the competition among different ionic species for the adsorption sites, but a quantitative modeling of the competition is not available yet. Deriving equation (5) assumes that all the available free surface sites of AIO are $\equiv\text{SOH}$ type. However, there must be other types of surface sites such as $\equiv\text{SO}^-$ and $\equiv\text{SOM}'$. The adsorption of a metal species on these sites would not cause any pH change as shown below;



We can not discriminate the equilibrium constants for reactions (7) and (8) from that for reaction (1). Thus, it should be noted that the apparent equilibrium constants, $K_{ad,app}$, calculated by equation (6) do not represent the equilibrium constants for individual reactions but indicate bulk adsorption properties of a metal component on AIO, as the term "apparent" implies.

SUMMARY AND CONCLUSIONS

The time-adsorption experiments indicate that the adsorption reactions of most of the trace metals, except Cr, Co, and Pb, with AIO from the coal mine drainage in Taebag area reach the equilibrium states within 400 mins. On the other hand, the pH-adsorption experiments show good linear relationships between the values of $\log(\Gamma/[M]_{aq})$ and pH for most of the trace elements except Pb. From these two experiments, we suspect the calculated $K_{ad,app}$ value for Pb, but may accept those for the other elements on AIO.

$K_{ad,app}$ and x for the adsorption reactions of Cr, Co, Ni, Cu, Zn, Cd, Pb, and U on AIO are calculated from the intercepts and slopes of the regression lines of $\log(\Gamma/[M]_{aq})$ versus pH. The calculated $K_{ad,app}$ of this study is much different from those obtained by simple experimental studies, but shows some similarity to those estimated from other natural systems. Despite the similarity in $K_{ad,app}$ between this study and the investigations for other natural systems, it is evident that $K_{ad,app}$ values of this study are uniquely appropriate only for the aquatic systems in Taebag coal mine area and thus, should be predetermined for adsorption modelling in the area. Moreover, for complete description of the trace metal behavior during the transport from mine seepage to the downstream, it is necessary to characterize the adsorption properties between the bottom sediments and the trace metals at site by site along the flow path, using the method as described in this study.

The calculated stoichiometric coefficients of proton, x , of this study are much smaller than generally accepted values. Although not certain, it may be caused by the competition among the different kinds of ionic species for the adsorption sites or by occurrence of other reactions not generating protons. The effects of the competition and presence of several reaction types can be evaluated only qualitatively with current knowledge.

The method used in this study may be similarly applied to other adsorption investigations and the results of this study will help construct an appropriate adsorption models. With the constructed models, one can describe the variations of trace element concentrations due to the adsorption in the aquatic systems, which is an essential part of the investigation

Table 4. The kind of the species and their fractions of each metal, which are obtained from MINTEQA2.

pH	Cr ³⁺	Cr(OH) ²⁺	CrOHSO ₄ ⁰	Cr(OH) ₂ ⁺	Cr(OH)	Cr(OH) ₄	CrO ₂	
2.84	0.945	0.035	0.01					
5.29	0.053	0.558	0.205	0.0181				
6.50		0.130	0.034	0.691	0.143			
7.41				0.367	0.620	0.014	0.035	
9.13				0.011	0.941			
pH	Co ²⁺	Co(OH) ₂ ⁰						
2.84	1	1.612E-9						
5.29	0.9937	0.62141E-3						
6.50	0	0.09090909						
7.41	9090909	0.83554						
9.13	0.1645	0.99992						
pH	Ni ²⁺	NiSO ₄ ⁰	NiCO ₃ ⁰	NiHCO ₃ ⁺	Ni(CO			
2.84	0.879	0.113						
5.29	0.852	0.135						
6.50	0.640	0.072	0.251	0.036				
7.41	0.162	0.031	0.790	0.014				
9.13			0.877		0.118			
pH	Cu ²⁺	CuOH ⁺	CuSO ₄ ⁰	CuHCO ₃ ⁺	CuCO ₃ ⁰	Cu(OH) ₂ ⁰		
2.84	0.873		0.118					
5.29	0.832		0.138	0.023				
6.50	0.574	0.013	0.068	0.108	0.163	0.074		
7.41	0.072	0.013	0.014	0.021	0.255	0.624		
9.13						0.992		
pH	Zn ²⁺	ZnOH ⁺	ZnSO ₄ ⁰	ZnHCO ₃ ⁺	ZnCO ₃ ⁰	Zn(OH) ₂ ⁰	Zn(CO ₃) ₂ ²⁻	
2.84	0.857		0.133					
5.29	0.830		0.158					
6.50	0.834		0.113	0.04				
7.41	0.682	0.014	0.156	0.049	0.089			
9.13	0.030	0.032			0.185	0.436	0.306	
pH	Cd ²⁺	CdCl ⁺	CdSO ₄ ⁰	CdHCO ₃ ⁺	CdCO ₃ ⁰			
2.84	0.647	0.222	0.123					
5.29	0.730	0.089	0.171					
6.50	0.772	0.050	0.129	0.037	0.010			
7.41	0.647	0.011	0.182	0.047	0.106			
9.13	0.108		0.032		0.840			
pH	Pb ²⁺	PbCl ⁺	PbSO ₄ ⁰	PbHCO ₃ ⁺	PbOH ⁺	PbCO ₃ ⁰	Pb(CO ₃) ₂ ²⁻	Pb(OH) ₂ ⁰
2.84	0.656	0.094	0.244					
5.29	0.636	0.032	0.290	0.028				
6.50	0.382	0.010	0.124	0.114	0.016	0.350		
7.41	0.072		0.040	0.033	0.026	0.825		
9.13					0.028	0.801	0.155	0.013
pH	UO ₂ ²⁺	UO ₂ SO ₄ ⁰	UO ₂ (SO ₄) ₂ ²⁻	UO ₂ OH ⁺	UO ₂ CO	UO ₂ (CO ₃) ₂ ²⁻	UO ₂ (CO ₃) ₃ ⁺	
2.84	0.726	0.252	0.014					
5.29	0.115	0.049		0.126	0.691			
6.50				0.013	0.466	0.515		
7.41					0.064	0.849	0.086	
9.13						0.179	0.821	

on the stream water quality affected by coal mine drainage.

ACKNOWLEDGMENT

The financial support from KOSEF grant #941-0400-011-2

is greatly acknowledged. We appreciate CEAM of EPA for providing us the computer program MINTEQA2. We are grateful to Dr. Park, Ms. Yun, and Mr. Park for allowing us to use the laboratory facilities of Korean Basic Science Center (KBSC). We also thank all the analysts of KBSC for

Table 5. Comparison of the $K_{ad,app}$ of this study with those reported by other investigators.

Metals	log $K_{ad,app}$			Reported by others	Reference ^a
	a	b	c		
Cr	-3.416	-4.37024	-4.65904	-	-
Co	-0.522	-1.47624	-1.76504	-4.2 ~ -3.87	(1)
Ni	0.305	-0.64924	-0.93804	-2.5 ~ 0.15	(4)
				-2.396 ~ -1.154	(5)
Cu	-0.344	-1.29824	-1.58704	-2.21	(1)
				-9.0 ~ -4.1	(2)
				-7.5 ~ -6.7	(3)
				0.6 ~ 2.85	(4)
Zn	-1.086	-2.04024	-2.32904	-4.22	(1)
				-17.5 ~ -16.9	(3)
				-1.98 ~ 0.97	(4)
				-1.85 ~ -0.608	(5)
Cd	1.122	0.167757	-1.12104	-4.91	(1)
				-11.2 ~ 5.1	(3)
				-2.9 ~ 0.43	(4)
				-2.652 ~ 1.41	(5)
Pb	0.925	-0.02924	-0.31804	-2.0 ~ -5.0	(3)
				0.3 ~ 4.71	(4)
				-0.42 ~ 0.752	(5)
U	3.994	3.039757	2.750962	-	-

* a: n=0.1, b: n=0.9, c: n=1.75 moles/mole Fe.
 @ (1): Kinniburgh, D.G. and Jackson, M.L.(1982).
 (2): Davis, J.A. and Leckie, J.O.(1982)
 (3): Benjamin, M.M. and Leckie, J.O.(1981)
 (4): Dzombak, D.A. and Morel, F.M.M (1990).

providing quality chemical compositional data.

REFERENCES

Allison, J.D., Brown, D.S., and Novo-Gradac, K.J., 1991, MINTEQA2/PRODEFA2, a geochemical assessment model for environmental systems: Version 3.0 user's manual, EPA/600/3-91/021.
 Anderson, P.R. and Benjamin, M.M., 1985, Effects of silicon on the crystallization and adsorption properties of ferric oxides, *Environmental Science and Technology*, v.19, p.1048-1053.
 Benjamin, M.M., 1983, Adsorption and surface precipitation of metals on amorphous iron oxyhydroxide, *Environmental Science and Technology*, v.17, p.686-692.
 Benjamin, M.M. and Leckie, J.O., 1981, Competitive adsorption of Cd, Cu, Zn and Pb on amorphous iron oxyhydroxide, *Journal of Colloid and Interface Science*, v.83, p.410-419.

Brown, K.P., 1991, Modelling of speciation, transport and transformation of metals from mine wastes, *Ecological Modelling*, v.57, p.65-89.
 Davis, J.A. and Kent, D.B., 1990, Surface complexation modelling in aqueous geochemistry, *Reviews in Mineralogy*, v.23, p.177-260.
 Davis, J.A. and Leckie, J.O., 1978, Surface ionization and complexation at the oxide/water interface, *Journal of Colloid and Interface Science*, v.67, p.90-107.
 Dzombak, D.A. and Morel, F.M.M., 1990, Surface complexation modelling: Hydrous ferric oxide, New York, Wiley, 393p.
 Faure, G., 1991, Principles and applications of inorganic geochemistry, New York, Macmillan Pub., 626p.
 Fuge, R., Laidlaw, I.M.S., Perkins, W.T., and Rogers, K.P., 1991, The influence of acidic mine and spoil drainage on water quality in the Mid-Wales Area, *Environmental Geochemistry and Health*, v.13, p.70-75.
 Helgeson, H.C., Delany, J.M., Nebitt, H.W., and Bird, D.K., 1978, Summary and critique of the thermodynamic properties of rockforming minerals, *American Journal of Science*, v.278A, 229p.
 Johnson, C.A., 1986, The regulation of trace element concentrations in river and estuarine waters contaminated with acid mine drainage: The adsorption of Cu and Zn on amorphous Fe oxyhydroxides, *Geochimica et Cosmochimica Acta*, v.50, p. 2433-2438.
 Kinniburgh, D.G. and Jackson, M.L., 1982, Concentration and pH dependence of calcium and zinc adsorption by iron hydrous oxide gel, *Soil Science Society of America Journal*, v.46, p.56-61.
 Livingstone, D.A., 1963, Chemical compositions of rivers and lakes, USGS Professional Paper, 440-G.
 Nordstrom, D.K., Jenne, E.A., and Averett, R.C., 1979, Heavy metal discharges into Shasta Lake and Keswick Reservoirs on the upper Sacramento River, California: A reconnaissance during low flow, *USGS Open File Report*, v.76-49, 25p.
 Robie, R.A., Hemingway, B.S., and Fisher, J.R., 1978, Thermodynamic properties of minerals and related substances at 298.15 K and 1 bar (10⁵ pascals) pressure and at higher temperatures, *USGS Bulletin*, v.1452, 456p.
 Sanden, P., 1991, Estimation and simulation of metal mass transport in an old mining area, *Water, Air and Soil Pollution*, v.57, p. 387-397.
 Tessier, A., Rapin, F., and Carignan, R., 1985, Trace metals in oxic lake sediments: Possible adsorption onto iron oxyhydroxides, *Geochimica et Cosmochimica Acta*, v.49, p.183-194.